28 Tibes R, Qiu Y, Lu Y *et al.* Reverse phase protein array: validation of a novel proteomic technology and utility for analysis of primary leukemia specimens and hematopoietic stem cells. *Mol Cancer Ther* 2006; **5**: 2512–21.
29 Kornblau SM, Tibes R, Qiu YH *et al.* Functional proteomic profiling of AML predicts response and survival. *Blood* 2009; **113**: 154–64.
30 Grote T, Siwak DR, Fritsche HA *et al.* Validation of reverse phase protein array for practical screening of potential biomarkers in serum and plasma: accurate detection of CA19-9 levels in pancreatic cancer. *Proteomics* 2008; **8**: 3051–60.
31 Tschopp J, Podack ER, Muller-Eberhard HJ. Ultrastructure of the membrane attack complex of complement: detection of the tetramolecular C9-polymerizing complex C5b-8. *Proc Natl Acad Sci U S A* 1982; **79**: 7474–8.
32 Gorter A, Meri S. Immune evasion of tumor cells using membrane-bound complement regulatory proteins. *Immunol Today* 1999; **20**: 576–82.

Supporting Information

Additional Supporting Information may be found in the online version of this article:

Fig. S1. Verification of reverse-phase plasma microarray (RPPM).

Please note: Wiley-Blackwell are not responsible for the content or functionality of any supporting materials supplied by the authors. Any queries (other than missing material) should be directed to the corresponding author for the article.

Research Article

Cancer Epidemiology, Biomarkers & Prevention

Reduced Plasma Level of CXC Chemokine Ligand 7 in Patients with Pancreatic Cancer

Junichi Matsubara[1,2], Kazufumi Honda[1], Masaya Ono[1], Yoshinori Tanaka[3], Michimoto Kobayashi[3], Giman Jung[3], Koji Yanagisawa[4], Tomohiro Sakuma[4], Shoji Nakamori[5], Naohiro Sata[6], Hideo Nagai[6], Tatsuya Ioka[7], Takuji Okusaka[8], Tomoo Kosuge[8], Akihiko Tsuchida[9], Masashi Shimahara[10], Yohichi Yasunami[11], Tsutomu Chiba[2], Setsuo Hirohashi[1], and Tesshi Yamada[1]

Abstract

Background: Early detection is essential to improve the outcome of patients with pancreatic cancer. A noninvasive and cost-effective diagnostic test using plasma/serum biomarkers would facilitate the detection of pancreatic cancer at the early stage.

Methods: Using a novel combination of hollow fiber membrane–based low-molecular-weight protein enrichment and LC-MS-based quantitative shotgun proteomics, we compared the plasma proteome between 24 patients with pancreatic cancer and 21 healthy controls (training cohort). An identified biomarker candidate was then subjected to a large blinded independent validation ($n = 237$, validation cohort) using a high-density reverse-phase protein microarray.

Results: Among a total of 53,009 MS peaks, we identified a peptide derived from CXC chemokine ligand 7 (CXCL7) that was significantly reduced in pancreatic cancer patients, showing an area under curve (AUC) value of 0.84 and a P value of 0.00005 (Mann–Whitney U test). Reduction of the CXCL7 protein was consistently observed in pancreatic cancer patients including those with stage I and II disease in the validation cohort ($P < 0.0001$). The plasma level of CXCL7 was independent from that of CA19-9 (Pearson's $r = 0.289$), and combination with CXCL7 significantly improved the AUC value of CA19-9 to 0.961 ($P = 0.002$).

Conclusions: We identified a significant decrease of the plasma CXCL7 level in patients with pancreatic cancer, and combination of CA19-9 with CXCL7 improved the discriminatory power of the former for pancreatic cancer.

Impact: The present findings may provide a new diagnostic option for pancreatic cancer and facilitate early detection of the disease. *Cancer Epidemiol Biomarkers Prev; 20(1); 160–71. ©2011 AACR.*

Introduction

Pancreatic adenocarcinoma is one of the most aggressive and lethal of diseases. The overall 5-year survival rate of patients with pancreatic cancer is less than 5%, which is the lowest among the more common cancers (1, 2), and the disease is the fifth leading cause of cancer death in Japan and the fourth in the United States, with greater than 23,000 estimated annual deaths in Japan and greater than 33,000 in the United States (3, 4). The 5-year survival rate of patients who were able to undergo surgical resection reaches 20% to 40% (5, 6), but the majority of pancreatic cancer patients have already developed lymph node and/or distant organ metastasis at their first clinical presentation, and only about 20% of patients are able to undergo radical resection (7, 8). The introduction of gemcitabine has significantly improved the overall survival of patients with unresectable pancreatic cancer, but their median survival period still remains about 6 months (9–11). These statistics

Authors' Affiliations: [1]Chemotherapy Division, National Cancer Center Research Institute, Tokyo; [2]Department of Gastroenterology and Hepatology, Kyoto University Graduate School of Medicine, Kyoto; [3]New Frontiers Research Laboratories, Toray Industries, Kamakura; [4]BioBusiness Group, Mitsui Knowledge Industry, Tokyo; [5]Department of Surgery, Osaka National Hospital, National Hospital Organization, Osaka; [6]Department of Surgery, Jichi Medical University, Shimotsuke; [7]Department of Hepatobiliary and Pancreatic Oncology, Osaka Medical Center for Cancer and Cardiovascular Diseases, Osaka; [8]Hepatobiliary and Pancreatic Oncology and Hepatobiliary and Pancreatic Surgery Divisions, National Cancer Center Hospital, Tokyo; [9]Third Department of Surgery, Tokyo Medical University, Tokyo; [10]Department of Oral Surgery, Osaka Medical College, Osaka; and [11]Department of Regenerative Medicine and Transplantation, Fukuoka University Faculty of Medicine, Fukuoka, Japan

Note: Supplementary data for this article are available at Cancer Epidemiology, Biomarkers & Prevention Online (http://cebp.aacrjournals.org/).

Corresponding Author: Tesshi Yamada, Chemotherapy Division, National Cancer Center Research Institute, 5-1-1 Tsukiji, Chuo-ku, Tokyo 104-0045, Japan. Phone: 81-3-3542-2511; Fax: 81-3-3547-6045. E-mail: tyamada@ncc.go.jp

doi: 10.1158/1055-9965.EPI-10-0397

demonstrate that early detection is essential for improving the outcome of patients with pancreatic cancer.

Computed tomography (CT), magnetic resonance imaging (MRI), and positron emission tomography (PET) are not cost-effective for the screening of pancreatic cancer because of the relatively low incidence of the disease. If a noninvasive and cost-effective screening test employing plasma/serum markers could be devised, it would significantly facilitate the early detection of pancreatic cancer. However, no biomarker suitable for screening of pancreatic cancer is currently available (12). CA19-9 is an established biomarker useful for the follow-up of pancreatic cancer patients receiving treatment, but has not been recommended for cancer screening because of its insufficient sensitivity and specificity (7, 13). Therefore, the discovery of a new biomarker that would be able to supplement CA19-9 has been anticipated.

Recently, advanced proteomic technologies based on mass spectrometry (MS) have been increasingly applied to studies of clinical samples to identify new biomarkers of various diseases (14) including pancreatic cancer (12, 15). It is anticipated that alterations in the protein content of clinical samples reflect the biological status of patients more directly than those in mRNA (16). We previously developed a new shotgun proteome platform, 2-Dimensional Image Converted Analysis of Liquid chromatography and mass spectrometry (2DICAL; ref. 17). 2DICAL is highly advantageous for clinical proteomics because of its high quantification accuracy and throughput. Using 2DICAL, we have been able to identify several plasma/serum biomarkers useful for cancer detection and therapy tailoring (18–20).

The serum/plasma proteome accumulates a large variety of disease-related alterations and is considered to be a rich source of biomarkers. However, for proteomic analysis of blood samples, the efficient depletion of a handful of particularly abundant proteins, such as albumin and immunoglobulin, has been challenging (21). Recently, we developed a novel method for the pretreatment of serum/plasma using the high-performance hollow fiber membrane (HFM) filtration technique (22). This method employs multistage filtration and cascaded cross-flow processes, enabling fully automated separation of proteins below a predetermined molecular weight (22). As the more abundant plasma proteins generally have relatively large molecular weights, they can be efficiently eliminated using the HFM technique.

To identify new biomarkers that might be useful for the early detection of patients with pancreatic cancer, we performed a comprehensive analysis of low-molecular-weight (LMW) plasma proteins in these patients using a combination of the HFM and 2DICAL techniques. A large variety of LMW proteins are known to be secreted from diseased tissues and can serve as good diagnostic biomarkers for various diseases (23, 24). Here, we report the identification and validation of an LMW chemotactic cytokine, CXC chemokine ligand 7 (CXCL7), as a novel biomarker for pancreatic cancer.

Patients and Methods

Plasma samples

Plasma samples were collected prospectively from 282 individuals (K. Honda, T. Okusaka, K. Felix, S. Nakamori, N. Sata, H. Nagai, et al., manuscript submitted) including healthy volunteers and newcomers to mainly departments of gastroenterology between August 2006 and October 2008 at the following 7 hospitals in Japan: National Cancer Center Hospital (NCCH), Osaka National Hospital (ONH), Jichi Medical School Hospital, Osaka Medical College (OMC), Tokyo Medical University Hospital (TMUH), Osaka Medical Center for Cancer and Cardiovascular Diseases, and Fukuoka University Hospital. This multi-institutional collaborative study group was organized by the "Third-Term Comprehensive Control Research for Cancer" conducted by the Ministry of Health, Labour and Welfare of Japan, and as part of the International Cancer Biomarker Consortium (25). The procedures used for collection and storage were kept uniform for all plasma samples.

The 282 plasma samples were split into 2 study sets (referred to as the training and validation cohorts). The training cohort comprised 45 individuals including patients with untreated pancreatic cancer at NCCH ($n = 19$) and TMUH ($n=5$), and healthy controls at NCCH ($n=2$), TMUH ($n=9$), OMC ($n=6$), and ONH ($n=4$). The validation cohort comprised 237 individuals including 140 patients with pancreatic cancer, 10 patients with chronic pancreatitis, and 87 healthy controls. All patients diagnosed as having pancreatic cancer had histologically or cytologically proven ductal adenocarcinoma. Demographic and laboratory data are summarized in Table 1. The staging of pancreatic cancer was in accordance with the TNM classification of the International Union against Cancer (UICC).

Blood was collected in a tube with EDTA at the time of diagnosis. The plasma was separated by centrifugation and frozen at −80°C until analysis. Samples showing macroscopic evidence of hemolysis were excluded from the current analysis. Written informed consent was obtained from every subject before blood collection. The protocol of this study was reviewed and approved by the institutional ethics committee boards of each participating institution.

Depletion of high-molecular-weight plasma proteins

The plasma samples of the training cohort were filtered through a 0.22-μm pore size filter. Five hundred microliters of the sample was diluted by adding 3.5 mL of 25 mmol/L of ammonium bicarbonate buffer (pH 8.0). The total 4 mL of the diluted plasma was processed as previously described (22). After 1 hour of fully automated operation, LMW proteins with molecular weights smaller than 60 kDa were recovered (Supplementary Fig. S1) and lyophilized.

The concentration of β2-microglobulin before and after HFM treatment was measured using an ELISA kit (Human Beta-2 Microglobulin ELISA Kit: Alpha Diagnostic Intl. Inc.) to ensure consistent recovery.

Table 1. Clinicopathologic characteristics of individuals in training and validation cohorts

	Training cohort (n = 45)			Validation cohort (n = 237)				
	Healthy control	Cancer	P	Healthy control	Cancer	P^f	Chronic pancreatitis	P^f
No. of patients	21	24		87	140		10	
Sex, n			0.205[a]			0.485[a]		0.487[a]
Male	17	15		56	83		8	
Female	4	9		31	57		2	
Age, y			<0.001			<0.001		0
mean (SD)	40 (13)	64 (7)		43 (16)	66 (10)		58 (13)	
Tumor location			NA			NA		NA
Head	–	14		–	59		–	
Body or tail	–	10		–	76		–	
Unknown	–	0		–	5		–	
Clinical stage			NA			NA		NA
I	–	1		–	5		–	
II	–	6		–	25		–	
III	–	4		–	40		–	
IV	–	13		–	70		–	
CA19-9 median, U/mL	5.5	1,109	<0.001	10.2	476	<0.001	5.2	0.06
>37.0 (ULN), no. of patients	2	19		4	110		0	
DUPAN-2 median, U/mL	12	540	<0.001	12	375	<0.001	25	<0.001
>150.0 (ULN), no. of patients	1	19		0	92		1	
CEA median, ng/mL	1.7	6.0	<0.001	1.7	3.5	<0.001	2.6	0.110
>5.0 (ULN), no. of patients	1	12		5	49		1	
Total bilirubin median, mg/dL	0.5	0.4	0.688	0.5	0.5	0.574	0.5	0.4
>1.2 (ULN), no. of patients	0	2		4	18		0	
CXCL7								
Mass spectrometry peak intensity[b], mean (SD)	332 (240)	138 (346)	<0.001[d]	–	–			
Protein intensity[c], mean (SD)	4.14 (0.18)	3.83 (0.28)	<0.001[e]	4.18 (0.14)	3.92 (0.28)	<0.001[e]	3.99 (0.10)	<0.001[e]

NOTE. Wilcoxon test was applied to assess differences in values.

Abbreviations: CEA, carcinoembryonic antigen; NA, not applicable; ULN, upper limit of normal.

[a]Calculated by Fisher's exact test.

[b]Intensity of the corresponding peak measured by quantitative mass spectrometry.

[c]Measured using reverse-phase protein microarrays (logarithmic variable).

[d]Calculated by Mann-Whitney U-test.

[e]Calculated by Welch's t test.

[f]Compared with healthy controls.

Liquid chromatography/mass spectrometry

The HFM-treated samples were digested with sequencing grade-modified trypsin (Promega) and analyzed in duplicate using a nano-flow high-performance liquid chromatography (HPLC; NanoFrontier nLC, Hitachi High-technologies) connected to an electrospray ionization quadrupole time-of-flight (ESI-Q-TOF) mass spectrometer (Q-Tof Ultima, Waters).

MS peaks were detected, normalized, and quantified using the in-house 2DICAL software package, as described previously (17). A serial identification (ID) number was applied to each of the MS peaks detected (1 to 53,009). The stability of LC-MS was monitored by calculating the correlation coefficient (CC) and coefficient of variance (CV) of every measurement. The mean CC ± SD and CV ± SD for all 53,009 peaks observed in the 45 duplicate runs were as high as 0.946 ± 0.042 and as low as 0.053 ± 0.010, respectively.

Protein identification by tandem MS (MS/MS)

Peak lists were generated using the Mass Navigator software package (version 1.2; Mitsui Knowledge Industry) and searched against the SwissProt database (downloaded on April 22, 2009) using the Mascot software package (version 2.2.1; Matrix Science). The search parameters used were as follows. A database of human proteins was selected. Trypsin was designated as the enzyme, and up to 1 missed cleavage was allowed. Mass tolerances for precursor and fragment ions were ± 0.6 Da and ± 0.2 Da, respectively. The score threshold was set to $P < 0.05$ based on the size of the database used in the search. If a peptide was matched to multiple proteins, the protein name with the highest Mascot score was selected.

Western blot analysis

Primary antibodies used were a rabbit polyclonal antibody against platelet basic protein (PBP) precursor (Sigma) and a mouse monoclonal antibody against human complement C3b-α (PROGEN). The anti-PBP antibody recognizes all the known cleaved forms of PBP including CTAP-III and NAP-2. Six microliters of 1:10 diluted plasma sample was separated by SDS-PAGE and electroblotted onto a polyvinylidene difluoride (PVDF) membrane. The membrane was then incubated with the primary antibody and subsequently with the relevant horseradish peroxidase (HRP)-conjugated anti-rabbit or anti-mouse IgG, as described previously (26, 27). Blots were developed using an enhanced chemiluminescence (ECL) detection system (GE Healthcare).

Reverse-phase protein microarray

The plasma samples were passed through IgY microbeads (Seppro-IgY12, Sigma-Aldrich) using an automated Magtration System SA-1 (Precision System Science) in accordance with the manufacturer's instructions to reduce the 12 most abundant plasma proteins. The flow-through portion was serially diluted 1:50, 1:100, 1:200, and 1:400 using a Biomek 2000 Laboratory Automation Robot (Beckman Coulter) and randomly plotted onto ProteoChip glass slides (Proteogen) in quadruplicate in a 6,144-spot/slide format using a Protein Microarrayer Robot (Kaken Geneqs). The spotted slides were incubated overnight with the anti-PBP precursor antibody and then with biotinylated anti-rabbit IgG (Vector Laboratories) and subsequently with streptavidin-HRP conjugate (GE Healthcare). The peroxidase activity was detected using the Tyramide Signal Amplification (TSA) Cyanine 5 System (PerkinElmer). The slides were counterstained with Alexa Fluor 546-labeled goat anti-human IgG (Invitrogen; spotting control).

The stained slides were scanned on a microarray scanner (InnoScan 700AL; Innopsys). Fluorescence intensity, determined as the mean value of quadruplicate samples, was determined using the Mapix software package (Innopsys). All determined intensity values were transformed into logarithmic variables.

The reproducibility of the reverse-phase protein microarray assay was determined by repeating the same experiment, as reported previously (28). A plasma sample after reduction of the 12 most abundant plasma proteins was serially diluted within a range of 25- to 6,400-fold. Each diluted sample was spotted in quadruplicate onto glass slides and blotted with the anti-PBP antibody. In a representative quality control experiment, the CC value was 0.980 between days and the median CV was 0.047 among the quadruplicates.

Multiplex assay

The levels of CXCL7 in plasma samples were measured using a Milliplex Human Cytokine/Chemokine panel III kit (Millipore) in accordance with the manufacturer's instructions.

Statistical analysis

Statistical significance of intergroup differences was assessed with the Wilcoxon test, Mann–Whitney U test, Welch's *t* test, or Fisher's exact test, as appropriate. The area under the curve (AUC) of the receiver-operating characteristic (ROC) was calculated for each marker to evaluate its diagnostic significance. A composite index of 2 markers was generated using the results of multivariate logistic regression analysis, which also enabled the calculation of sensitivity, specificity, and the ROC curve. Statistical analyses were performed using an open-source statistical language R (version 2.7.0) with the optional module Design package.

Results

Plasma proteins associated with pancreatic cancer

A plasma sample from 1 healthy volunteer was processed 3 times using the HFM filtration technique. The concentration of β2-microglobulin before and after HFM treatment was measured. The recovery rates were

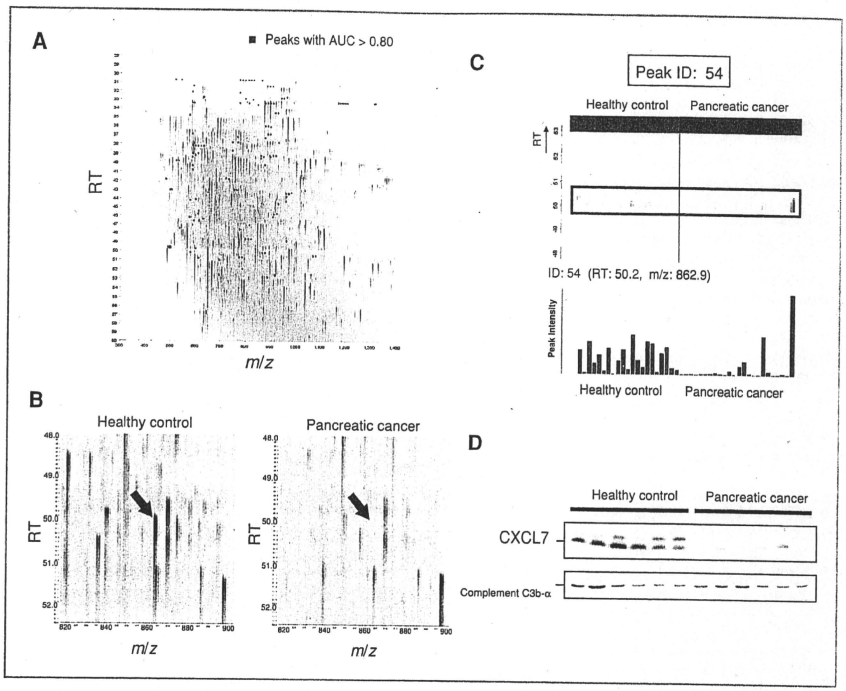

Figure 1. A, 2-dimensional display of all (>53,000) the MS peaks with *m/z* values along the *x*-axis and RT of LC along the *y*-axis. The peaks are displayed with a bin size of 1.0 *m/z*. The 140 MS peaks whose mean intensity of duplicates that distinguished pancreatic cancer patients from healthy controls with AUC values of greater than 0.800 are highlighted in red. B, CXCL7-derived MS peak (ID 54, at 863 *m/z* and 50.2 minutes) in representative patients from the cancer and control groups. C, CXCL7-derived MS peak (ID 54) in 45 duplicate LC-MS runs [patients with pancreatic cancer (red) and healthy controls (blue)] aligned along the RT of LC. Columns represent the mean intensity of duplicates (bottom). D, detection of CXCL7 and complement C3b-α (loading control) by Western blotting. Multiple bands for CXCL7 indicate the presence of proteolytic products.

25.11%, 25.73%, and 29.16%, respectively. Although the rates were seemingly low, the HFM treatment was highly reproducible with a CV of 0.081 and the amount of β2-microglobulin relative to total protein was increased 150 to 200-fold after HFM treatment.

To identify a diagnostic biomarker for pancreatic cancer, we compared the plasma LMW proteome between 24 patients with pancreatic cancer and 21 healthy controls (training cohort) using 2DICAL. Among a total of 53,009 independent MS peaks detected within the range 250 to 1,600 *m/z* and within a time range of 20 to 70 minutes, we found that 140 peaks had discriminatory ability with a AUC of above 0.800. Figure 1A is a representative 2-dimensional view of all the MS peaks displayed with *m/z* along the *x*-axis and the retention time (RT) of LC along the *y*-axis.

Twenty-five MS/MS spectra acquired from those 140 peaks were recurrently matched to 10 proteins in the database with a Mascot score of greater than 30 (Supplementary Table S1). Notably, one MS peak (ID 54) matched the amino acid sequence of the *CXCL7* gene product (Swiss-Prot_P02775) with the highest score of 99.6 (Supplementary Fig. S2). Figure 1B shows the CXCL7-derived MS peak (ID 54, at 863 *m/z* and 50.2 minutes) that appeared in a representative pancreatic cancer patient and a healthy individual. Figure 1C demonstrates the distribution of the MS peak (ID 54) in patients with pancreatic cancer (red) and healthy controls (blue) in the training cohort (AUC = 0.839; $P = 4.54 \times 10^{-5}$; Mann–Whitney U test). The differential expression and identification of CXCL7 was confirmed by immunoblotting (Fig. 1D).

Validation of reduced CXCL7 in pancreatic cancer patients

The level of plasma CXCL7 was quantified in 12 patients with pancreatic cancer and 12 healthy individuals in the training cohort using multiplex assay. Consistent with 2DICAL, CXCL7 was found to be significantly decreased in patients with pancreatic cancer (mean ± SD, 744 ± 182 ng/mL) in comparison with healthy controls (1,355 ± 386 ng/mL; $P = 0.0003$). To further verify and validate the reduction of plasma CXCL7 in pancreatic cancer patients, 280 plasma samples [including 43 samples from the training cohort and new 237 samples (validation cohort)] were randomly plotted into a reverse-phase protein microarray and blotted with anti-PBP antibody (Fig. 2). Two samples from healthy controls in the training cohort were excluded due to an insufficient sample volume. Quadruplicate spots for representative cases and controls with high and low levels of CXCL7 are shown in the right panels of Figure 2.

The results of reverse-phase protein microarray were well correlated with those of multiplex assay (Pearson's $r = 0.65$; $P = 0.0006$; Supplementary Fig. S3). Microarray analysis also showed a significant reduction of the plasma CXCL7 level in the pancreatic cancer patients of the training cohort ($P = 5.96 \times 10^{-5}$; Welch's t test; Fig. 3A and Table 1) with an AUC value of 0.872 (95% CI: 0.732–0.951; Fig. 3B). The reduction of plasma CXCL7 was further validated in a larger independent cohort (validation cohort; $P = 1.40 \times 10^{-16}$; Fig. 3C and AUC value of 0.850, 95% CI: 0.792–0.895; Fig. 3B). Because there was a difference in age distribution between the cancer patients and healthy controls of the validation cohort (Table 1), we performed a subgroup analysis of 79 pancreatic cancer patients (median age, 61) and 20 healthy controls (median age, 60) aged 50 to 70 years. The reduction of plasma CXCL7 in patients with pancreatic cancer was statistically significant even in this subgroup ($P = 0.0001$), indicating that the decrease of the CXCL7 level was not merely due to the difference of age distribution between the pancreatic cancer patients and controls.

CXCL7 was significantly reduced in patients with any stage of pancreatic cancer (Table 2), including those with stage I (<0.001) and II (<0.001) disease. The significant alteration evident in early-stage patients indicated that the reduction of plasma CXCL7 is an early event in pancreatic carcinogenesis and may precede the development of cancer. The persistent presence of inflammation is known to promote carcinogenesis in various organs, and chronic pancreatitis is suspected to be one a precancerous condition for pancreatic cancer, although opinions on this issue vary. We measured the plasma level of CXCL7 in a small number of patients diagnosed as having chronic pancreatitis ($n = 10$) using the reverse-phase protein microarray (Table 1). The CXCL7 levels in patients with chronic pancreatitis were significantly lower than those in healthy controls ($P = 0.0002$), but slightly higher than those in patients with pancreatic cancer ($P = 0.095$; Fig. 3C).

Complementation of CA19-9 by CXCL7

CA19-9 is an established biomarker that has long been used for the diagnosis of pancreatic cancer. We found that the levels of CXCL7 and CA19-9 were not mutually correlated (Pearson's $r = 0.289$) and that combination with CXCL7 significantly improved the ability of CA19-9 to distinguish patients with pancreatic cancer from healthy controls: the AUC value improved to 0.965 (95% CI: 0.865–0.994) in the training cohort ($P = 0.026$) and to 0.961 (0.932–0.979) in the validation cohort ($P = 0.002$; Fig. 3D). The AUC values of CA19-9 in the 2 cohorts (Fig. 3D) were comparable with those reported previously (29–31).

Even among individuals with normal levels of CA19-9 (<37 U/mL; a cutoff value widely used in clinical practice), CXCL7 was significantly reduced in pancreatic cancer patients in both the training [$P = 0.014$ and AUC = 0.853 (95% CI: 0.650–0.957; Fig. 4A and B)] and validation [$P < 0.0001$ and AUC = 0.834 (95% CI: 0.747–0.899; Fig. 4B and C)] cohorts.

Because of the low prevalence of pancreatic cancer, any screening biomarker must have high specificity (32). The sensitivity/specificity of CA19-9 (cutoff: 37 U/mL) were 79%/89% in the training cohort and 79%/95% in the validation cohort, consistent with previous reports (32). If we defined the cutoff for CXCL7 as a level at which 95% of healthy individuals would be excluded, 83% of pancreatic cancer patients in the training cohort and 84% in the validation cohort would be detected using the combination of CXCL7 and CA19-9 (Supplementary Table S2).

Discussion

Early detection and subsequent radical surgical resection would most likely provide a chance of cure for patients with pancreatic cancer (7). However, patients with early-stage pancreatic cancer are generally asymptomatic and have little opportunity to undergo imaging and/or other diagnostic procedures until their disease becomes advanced. If a sensitive, but minimally invasive and cost-effective, plasma/serum test were available, it would be effective for alerting patients with early pancreatic cancer and offer them a chance to receive prompt and effective medical attention. In the present study, we compared the plasma LMW proteome between patients with pancreatic cancer and healthy controls using a new proteome platform, 2DICAL (Fig. 1), and found a significant decrease of the plasma CXCL7 level in patients with pancreatic cancer (Fig. 1B and C). The result of quantitative LC-MS was then verified using 3 different methods: immunoblotting (Fig. 1D), multiplex, and reverse-phase protein microarray (Figs. 2 and 3) assays. We further validated the significant decrease of CXCL7 in a larger independent cohort (validation cohort). The level of plasma CXCL7 was confirmed to be decreased reproducibly in patients with pancreatic cancer including those with Stage I and II disease (Table 2). CXCL7 did not

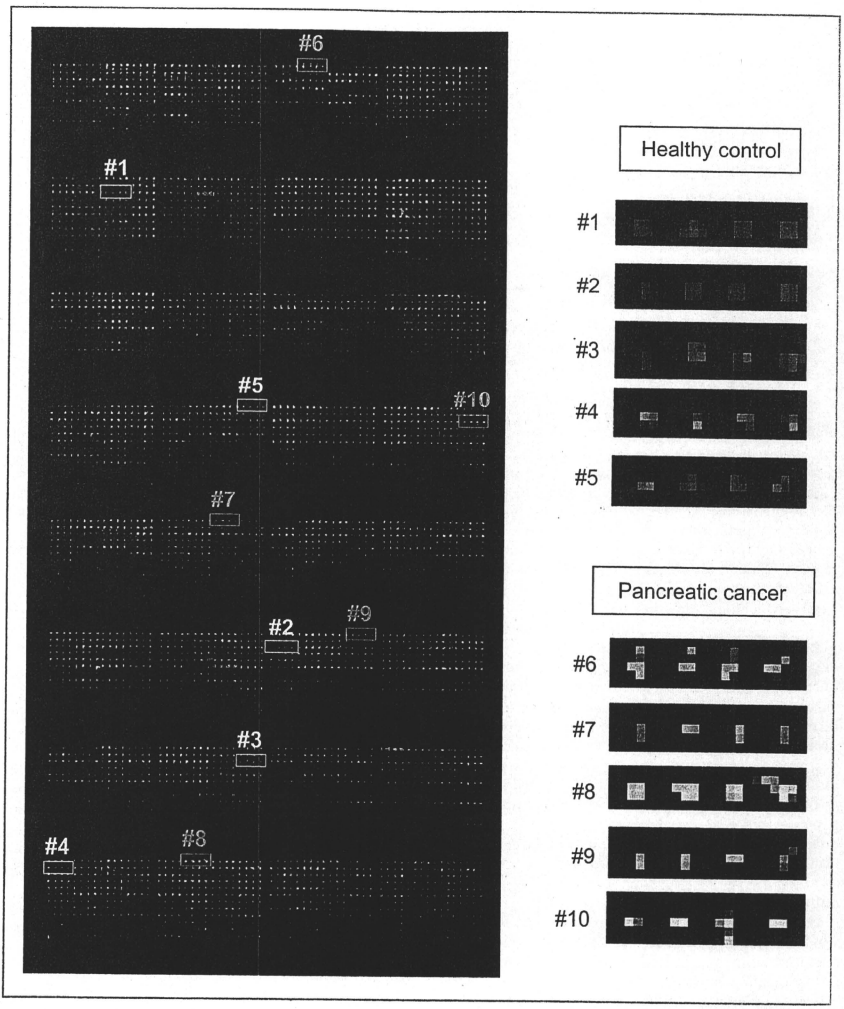

Figure 2. Image of a representative reverse-phase protein microarray slide stained with anti-PBP antibody (left). Samples were randomly assigned, and quadruplicate spots from representative patients with high and low levels of CXCL7 were extracted (right).

surpass the sensitivity of CA19-9, but was able to supplement it. Combination with CXCL7 significantly improved the sensitivity of CA19-9 (Fig. 3D and Supplementary Table S2).

In addition to 2DICAL, we utilized 2 state-of-the-art proteome technologies. The proteome analysis of plasma/serum samples has been hampered by the prominence of a handful of abundant proteins such as

Table 2. Plasma CXCL7 level according to clinical stage of pancreatic cancer

	Pancreatic cancer patients				Healthy controls
	Stage I	Stage II	Stage III	Stage IV	
Training cohort					
No. of cases	1	6	4	13	19[b]
CXCL7[a], mean (SD)	3.67 (-)	3.93 (0.24)	3.75 (0.17)	3.82 (0.33)	4.14 (0.18)
P (vs. healthy controls)	0.01	0.01	<0.001	<0.001	
Validation cohort					
No. of cases	5	25	40	70	87
CXCL7[a], mean (SD)	3.89 (0.34)	3.96 (0.25)	4.02 (0.18)	3.86 (0.32)	4.18 (0.14)
P (vs. healthy controls)	<0.001	<0.001	<0.001	<0.001	

NOTE. Welch's *t* test was applied to assess differences in values.

[a]Measured using reverse-phase protein microarrays.

[b]Two patients whose samples were not available for reverse-phase protein microarrays were excluded.

albumin and immunoglobulin. It is anticipated that the remaining proteins contain an unexplored archive of disease-driven information, but account for only about 1% of the entire human plasma proteome (24). To reduce the complexity of the plasma proteome, we used HFM filtration technology. Our HFM devise can separate and concentrate LMW plasma proteins in a fully automated manner (22) and allows identification of any biomarker candidate that is present at a level of 1 μg/mL. This discovery justifies the future application of the HFM system to more detailed proteome studies aimed at plasma/serum biomarker discovery. The other technology we employed is high-density reverse-phase protein microarray. The protein content of any human sample varies according to the individual, and therefore it is essential to distinguish biomarker candidates from simple interindividual heterogeneity. However, such distinction is possible only by comparing a statistically sufficient number of cases and controls. Our high-density protein microarrays require a minimal sample volume of the nanoliter order and make it possible to measure the quantity of any candidate biomarker protein in a statistically sufficient number of cases and controls (>300 samples; ref. 28) for judgment of its clinical potential in a single experiment.

LMW chemotactic cytokines have been implicated in various biological processes, such as leukocyte migration, angiogenesis, hematopoiesis, atherosclerosis, and cancer migration and metastasis. CXCL7, also known as PBP, is one of the members of the angiogenic ELR^+ CXC chemokine family (33). It is reportedly produced and stored in platelets, monocytes, neutrophils, and megakaryocytes. Secreted CXCL7 binds to CXC chemokine receptor 2 (CXCR2) on endothelium and mediates angiogenesis through activation of the Ras/Raf/mitogen-activated protein kinase (MAPK) and PI3K/AKT/mTOR signaling pathways (33, 34). The histology of pancreatic ductal adenocarcinoma is often characterized by hypovascularization. The reduction of circulating CXCL7 in patients with pancreatic cancer may play a certain role in the suppression of angiogenesis.

Recently, reduction in the level of serum CXCL7 has been reported to be a biomarker for advanced myelodysplastic syndrome (35). In contrast, CXCL7 is increased in the pulmonary venous blood of lung cancer patients and is significantly decreased after curative surgical resection of the lung lesions. Of particular interest is the fact that the increment of CXCL7 is detectable several months before diagnosis of lung cancer (36). We observed a reduction of CXCL7 in 10 patients with chronic pancreatitis; but, examination of a larger number of patients will be needed before any definite conclusion can be reached.

CXCL7 is N-terminally truncated by cathepsin G-like enzymes and converted to other types of chemokines with distinct functions such as connective tissue-activating peptide III (CTAP-III) and neutrophil-activating peptide 2 (NAP-2; refs. 37, 38). One possible explanation for the reduction of plasma CXCL7 in patients with pancreatic cancer is degradation by certain exoproteases (39). Matrix metalloproteinase-9 (MMP9) has been reported to degrade CXC chemokines (40). MMP9 is often upregulated in pancreatic cancer cells and secreted into plasma (41). However, in this study, the precise molecular mechanisms behind the reduction of plasma CXCL7 in patients with pancreatic cancer remained unexplained.

Because the process of pancreatic carcinogenesis is probably mediated by various molecular pathways (42), the diagnosis of pancreatic cancer using a single biomarker may not be realistic, and a combination of different biomarkers with distinct spectra would appear to be a more realistic alternative. CA19-9 is the most widely used serum biomarker for pancreatic cancer; but, its sensitivity and specificity have been recognized

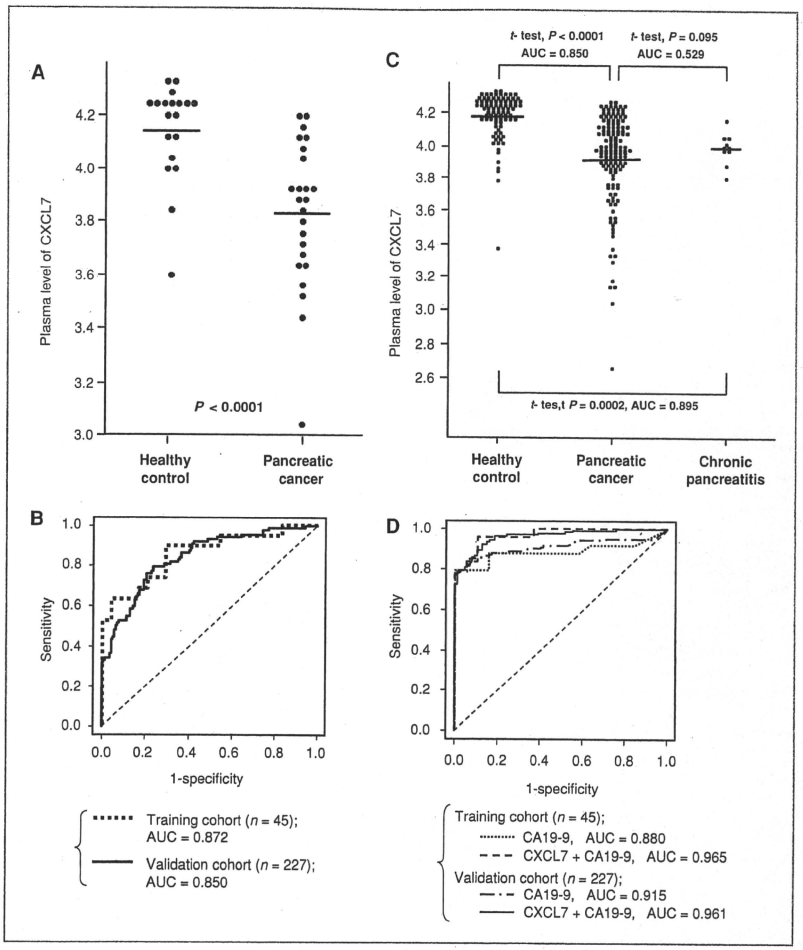

Figure 3. A and C, plasma levels (in arbitrary units) of CXCL7 in healthy controls, patients with pancreatic cancer, and patients with chronic pancreatitis in the training (A) and validation (C) cohorts. Horizontal lines represent the average levels of CXCL7. B, ROC analyses for the discriminatory value of CXCL7 in the training (dotted line) and validation (solid line) cohorts. D, ROC analyses for the discriminatory value of CA19-9 and the composite index of CA19-9 and CXCL7 in the training and validation cohorts.

to be unsatisfactory for pancreatic cancer screening (7, 12). We demonstrated that CXCL7 significantly improved the discriminatory ability of CA19-9, and this improvement was reproducibly validated in a large multi-institutional cohort. However, further independent validation by other investigators is still mandatory before its clinical application can be warranted (15, 29–31, 43).

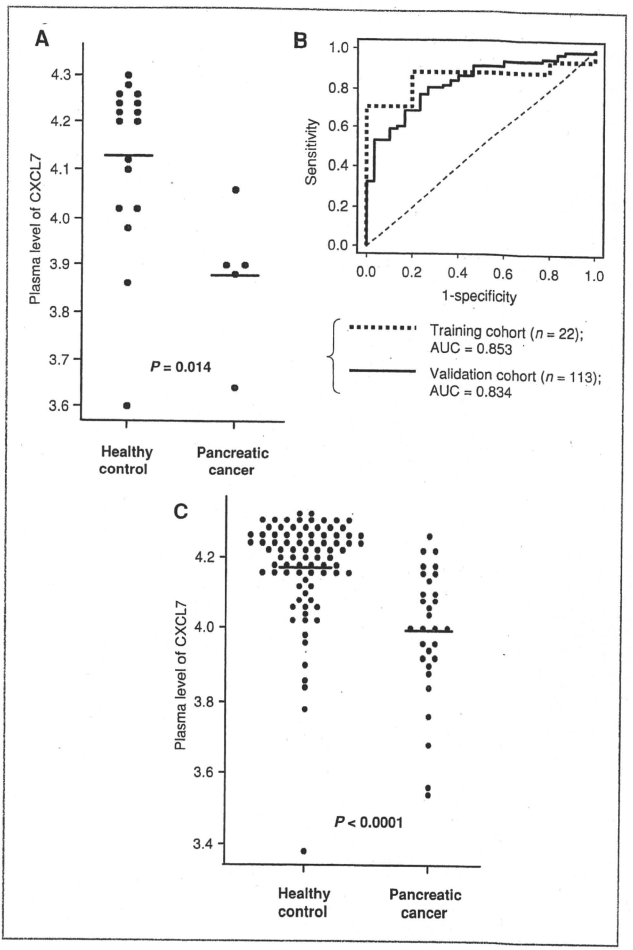

Figure 4. A and C, plasma levels of CXCL7 in healthy controls (left) and patients with pancreatic cancer (right) with the normal levels of CA19-9 (<37 U/mL) in the training (A) and validation (C) cohorts. Horizontal lines represent the average levels of CXCL7. B, ROC analyses of CXCL7 for discrimination between pancreatic cancer patients and healthy controls with normal levels of CA19-9 (<37 U/mL) in the training (dotted line) and validation (solid line) cohorts.

The primary goal of the present study was to discover new biomarkers useful for the early detection of pancreatic cancer in an asymptomatic population. Aberrations of circulating CXCL7 have also been reported in other premalignant conditions. The present study has not only explored the utility of CXCL7 as a biomarker, but also provided a novel insight into the chemokine-mediated reactions that occur during early carcinogenesis.

Disclosure of Potential Conflicts of Interest

These sponsors had no role in the design of the study, the collection of the data, the analysis and interpretation of the data, the decision to submit the manuscript for publication, or the writing of the manuscript.

Acknowledgment

We thank Ms. Ayako Igarashi, Ms. Tomoko Umaki, and Ms. Yuka Nakamura for their technical assistance.

Grant Support

Program for Promotion of Fundamental Studies in Health Sciences conducted by the National Institute of Biomedical Innovation of Japan, the Third-Term Comprehensive Control Research for Cancer and Research on Biological Markers for New Drug Development conducted by the Ministry of Health and Labor of Japan.

The costs of publication of this article were defrayed in part by the payment of page charges. This article must therefore be hereby marked *advertisement* in accordance with 18 U.S.C. Section 1734 solely to indicate this fact.

Received April 15, 2010; revised October 22, 2010; accepted November 28, 2010; published OnlineFirst December 8, 2010.

References

1. Jemal A, Murray T, Samuels A, Ghafoor A, Ward E, Thun MJ. Cancer statistics, 2003. CA Cancer J Clin 2003;53:5–26.
2. Michl P, Pauls S, Gress TM. Evidence-based diagnosis and staging of pancreatic cancer. Best Pract Res Clin Gastroenterol 2006;20:227–51.
3. Ministry of Health, Labour and Welfare. Japanese Government: vital statistics of Japan2009. Available from: http://ganjoho.ncc.go.jp/professional/statistics/odjrh3000000hwsa-att/cancer_mortality(1958-2008).xls.
4. American Cancer Society. Cancer Facts and Figures2007. Atlanta, GA: American Cancer Society; 2007. p. 16–7.
5. Nitecki SS, Sarr MG, Colby TV, van Heerden JA. Long-term survival after resection for ductal adenocarcinoma of the pancreas. Is it really improving?Ann Surg 1995;221:59–66.
6. Tsuchiya R, Noda T, Harada N, Miyamoto T, Tomioka T, Yamamoto K, et al. Collective review of small carcinomas of the pancreas. Ann Surg 1986;203:77–81.
7. DiMagno EP, Reber HA, Tempero MA. AGA technical review on the epidemiology, diagnosis, and treatment of pancreatic ductal adenocarcinoma. American Gastroenterological Association. Gastroenterology 1999;117:1464–84.
8. Nieto J, Grossbard ML, Kozuch P. Metastatic pancreatic cancer 2008: is the glass less empty?Oncologist 2008;13:562–76.
9. Burris HA 3rd, Moore MJ, Andersen J, Green MR, Rothenberg ML, Modiano MR, et al. Improvements in survival and clinical benefit with gemcitabine as first-line therapy for patients with advanced pancreas cancer: a randomized trial. J Clin Oncol 1997;15:2403–13.
10. Poplin E, Feng Y, Berlin J, Rothenberg ML, Hochster H, Mitchell E, et al. Phase III, randomized study of gemcitabine and oxaliplatin versus gemcitabine (fixed-dose rate infusion) compared with gemcitabine (30-minute infusion) in patients with pancreatic carcinoma E6201: a trial of the Eastern Cooperative Oncology Group. J Clin Oncol 2009;27:3778–85.
11. NCCN Clinical Practice Guidelines in Oncology: Pancreatic Adenocarcinoma V.1. National Comprehensive Cancer Network; 2009.
12. Goggins M. Molecular markers of early pancreatic cancer. J Clin Oncol 2005;23:4524–31.
13. Goggins M, Canto M, Hruban R. Can we screen high-risk individuals to detect early pancreatic carcinoma?J Surg Oncol 2000;74:243–8.
14. Hanash S. Disease proteomics. Nature 2003;422:226–32.
15. Grantzdorffer I, Carl-McGrath S, Ebert MP, Rocken C. Proteomics of pancreatic cancer. Pancreas 2008;36:329–36.
16. Yamaguchi U, Nakayama R, Honda K, Ichikawa H, Hasegawa T, Shitashige M, et al. Distinct gene expression-defined classes of gastrointestinal stromal tumor. J Clin Oncol 2008;26:4100–8.
17. Ono M, Shitashige M, Honda K, Isobe T, Kuwabara H, Matsuzuki H, et al. Label-free quantitative proteomics using large peptide data sets generated by nanoflow liquid chromatography and mass spectrometry. Mol Cell Proteomics 2006;5:1338–47.
18. Matsubara J, Ono M, Negishi A, Ueno H, Okusaka T, Furuse J, et al. Identification of a predictive biomarker for hematologic toxicities of gemcitabine. J Clin Oncol 2009;27:2261–8.
19. Negishi A, Ono M, Handa Y, Kato H, Yamashita K, Honda K, et al. Large-scale quantitative clinical proteomics by label-free liquid chromatography and mass spectrometry. Cancer Sci 2009;100:514–9.
20. Ono M, Matsubara J, Honda K, Sakuma T, Hashiguchi T, Nose H, et al. Prolyl 4-hydroxylation of alpha-fibrinogen: a novel protein modification revealed by plasma proteomics. J Biol Chem 2009;284:29041–9.
21. Anderson NL, Anderson NG. The human plasma proteome: history, character, and diagnostic prospects. Mol Cell Proteomics 2002;1:845–67.
22. Tanaka Y, Akiyama H, Kuroda T, Jung G, Tanahashi K, Sugaya H, et al. A novel approach and protocol for discovering extremely low-abundance proteins in serum. Proteomics 2006;6:4845–55.
23. Kennedy S. The role of proteomics in toxicology: identification of biomarkers of toxicity by protein expression analysis. Biomarkers 2002;7:269–90.
24. Tirumalai RS, Chan KC, Prieto DA, Issaq HJ, Conrads TP, Veenstra TD. Characterization of the low molecular weight human serum proteome. Mol Cell Proteomics 2003;2:1096–103.
25. Available from: http://www.fhcrc.org/science/international_biomarker/.
26. Honda K, Yamada T, Hayashida Y, Idogawa M, Sato S, Hasegawa F, et al. Actinin-4 increases cell motility and promotes lymph node metastasis of colorectal cancer. Gastroenterology 2005;128:51–62.
27. Idogawa M, Yamada T, Honda K, Sato S, Imai K, Hirohashi S. Poly (ADP-ribose) polymerase-1 is a component of the oncogenic T-cell factor-4/beta-catenin complex. Gastroenterology 2005;128:1919–36.
28. Matsubara J, Ono M, Honda K, Negishi A, Ueno H, Okusaka T, et al. Survival prediction for pancreatic cancer patients receiving gemcitabine treatment. Mol Cell Proteomics 2010;9:695–704.
29. Fiedler GM, Leichtle AB, Kase J, Baumann S, Ceglarek U, Felix K, et al. Serum peptidome profiling revealed platelet factor 4 as a potential discriminating Peptide associated with pancreatic cancer. Clin Cancer Res 2009;15:3812–9.
30. Koopmann J, Zhang Z, White N, Rosenzweig J, Fedarko N, Jagannath S, et al. Serum diagnosis of pancreatic adenocarcinoma using surface-enhanced laser desorption and ionization mass spectrometry. Clin Cancer Res 2004;10:860–8.
31. Koopmann J, Buckhaults P, Brown DA, Zahurak ML, Sato N, Fukushima N, et al. Serum macrophage inhibitory cytokine 1 as a marker of pancreatic and other periampullary cancers. Clin Cancer Res 2004;10:2386–92.
32. Rhodes JM. Usefulness of novel tumour markers. Ann Oncol 1999;10Suppl 4:118–21.
33. Strieter RM, Burdick MD, Mestas J, Gomperts B, Keane MP, Belperio JA. Cancer CXC chemokine networks and tumour angiogenesis. Eur J Cancer 2006;42:768–78.
34. Heidemann J, Ogawa H, Dwinell MB, Rafiee P, Maaser C, Gockel HR, et al. Angiogenic effects of interleukin 8 (CXCL8) in human intestinal microvascular endothelial cells are mediated by CXCR2. J Biol Chem 2003;278:8508–15.
35. Aivado M, Spentzos D, Germing U, Alterovitz G, Meng XY, Grall F, et al. Serum proteome profiling detects myelodysplastic syndromes and identifies CXC chemokine ligands 4 and 7 as markers for advanced disease. Proc Natl Acad Sci USA 2007;104:1307–12.
36. Yee J, Sadar MD, Sin DD, Kuzyk M, Xing L, Kondra J, et al. Connective tissue-activating peptide III: a novel blood biomarker for early lung cancer detection. J Clin Oncol 2009;27:2787–92.
37. Ehlert JE, Ludwig A, Grimm TA, Lindner B, Flad HD, Brandt E. Down-regulation of neutrophil functions by the ELR(+) CXC chemokine platelet basic protein. Blood 2000;96:2965–72.
38. Pillai MM, Iwata M, Awaya N, Graf L, Torok-Storb B. Monocyte-derived CXCL7 peptides in the marrow microenvironment. Blood 2006;107:3520–6.

39. Villanueva J, Shaffer DR, Philip J, Chaparro CA, Erdjument-Bromage H, Olshen AB, et al. Differential exoprotease activities confer tumor-specific serum peptidome patterns. J Clin Invest 2006;116:271–84.
40. Van Den Steen PE, Proost P, Wuyts A, Van Damme J, Opdenakker G. Neutrophil gelatinase B potentiates interleukin-8 tenfold by aminoterminal processing, whereas it degrades CTAP-III, PF-4, and GRO-alpha and leaves RANTES and MCP-2 intact. Blood 2000;96:2673–81.
41. Tian M, Cui YZ, Song GH, Zong MJ, Zhou XY, Chen Y, et al. Proteomic analysis identifies MMP-9, DJ-1 and A1BG as overexpressed proteins in pancreatic juice from pancreatic ductal adenocarcinoma patients. BMC Cancer 2008;8:241.
42. Gansauge S, Gansauge F, Beger HG. Molecular oncology in pancreatic cancer. J Mol Med 1996;74:313–20.
43. Honda K, Hayashida Y, Umaki T, Okusaka T, Kosuge T, Kikuchi S, et al. Possible detection of pancreatic cancer by plasma protein profiling. Cancer Res 2005;65:10613–22.

Hepatocellular carcinomas can develop in simple fatty livers in the setting of oxidative stress

Sir,

It is doubtless that non-alcoholic fatty liver disease (NAFLD) has become a critical public health issue in most developed countries.[1] In addition to its close association with metabolic disorders and cardiovascular events, NAFLD itself can progress to life-threatening liver diseases, cirrhosis and hepatocellular carcinoma (HCC).[1,2] Surprisingly, recent clinical observations have revealed that HCC can develop in non-cirrhotic, but steatotic livers without significant fibrosis.[3,4] In the reports, authors emphasised the importance of underlying metabolic disorders and oxidative stress in hepatocarcinogenesis in such NAFLD cases.

We herein report a case of NAFLD complicated by HCC, in which the potential contribution of oxidative stress to hepatocarcinogenesis in NAFLD has been further strongly suggested.

In May 2006, a 72-year-old obese Japanese man was admitted to the National Hospital Organization Osaka National Hospital, Japan, because of a hepatic nodule. The patient had a 5 year medical history of hypertension and fatty liver. He underwent an operation for abdominal aortic aneurysm in April 2004, and had since been an outpatient. Follow-up abdominal ultrasonography showed, in addition to hepatic steatosis, a nodular lesion approximately 2 cm in diameter in the left lobe of the liver. The hepatic nodule had been growing larger, and findings of computed tomography (CT) strongly suggested that it was HCC (Fig. 1).

On admission, he appeared to be healthy except for obesity, and the laboratory test results showed normal serum levels of transaminases and negativity for hepatitis B and C viruses. After the examinations, under the tentative diagnosis of HCC, a surgical operation was performed to remove the left lobe of the liver. The cut surface of the liver sample was smooth and yellowish-brown, and demonstrated the clearly circumscribed nodule 5 cm in diameter (Fig. 2). Histological examination revealed that the nodular lesion was well-differentiated HCC (Fig. 3A), and the background hepatic disorder was simple steatosis without inflammation and fibrosis (Fig. 3B). Routine pathological examination couldn't detect any causative factors in hepatocarcinogenesis, such as iron overload. However, an immunohistochemical analysis revealed that as well as tumour cells, a few non-tumourous hepatocytes showed immunoreactivity for anti-oxidised phosphatidylcholine (oxPC; Fig. 3A,B insets), a marker of

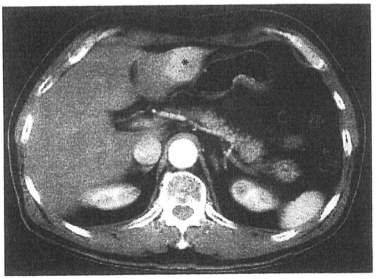

Fig. 1 Findings of computed tomography. A hypervascular nodule is seen in the left lobe of the liver (asterisk).

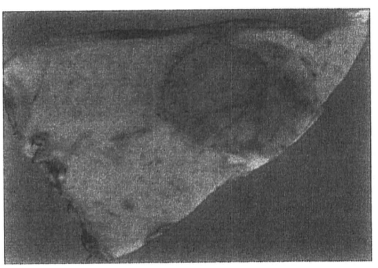

Fig. 2 The cut-surface of the liver sample. A well-circumscribed nodular lesion 5 cm in diameter is present.

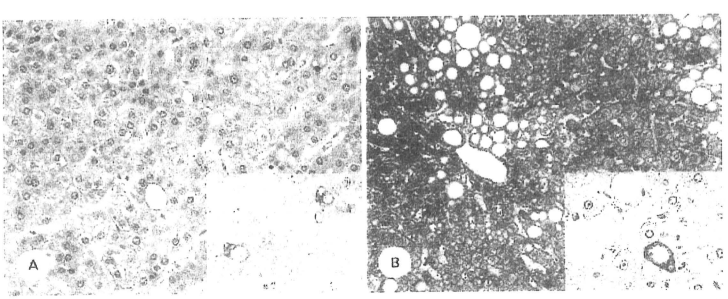

Fig. 3 Microscopic findings of the liver sample. (A) The hepatic nodule consists of well-differentiated HCC (H&E). (B) A background liver condition is simple steatosis without fibrosis (Azan-Mallory stain for collagen). Insets: steatotic liver cells of both tumourous and non-tumourous portions are positive for oxPC (immunoperoxidase with anti-oxPC).

oxidative cellular injury.[5] The immunoreactivity was found restrictively in steatotic cells in both tumourous and non-tumourous portions. It suggested that the steatosis-related oxidative hepatocellular injury had persisted and had played a certain role in the development of HCC. His postoperative course was uneventful and he was discharged. Follow-up examinations have been done every 3 months, resulting in no evidence of tumour recurrence. When last seen, in December 2009, he was well.

Like the present case, HCC can develop in non-inflammatory, non-fibrotic, but steatotic livers. A previous case report of HCC arising in the absence of advanced NAFLD emphasised the potential roles for metabolic factors (diabetes, hypertension, obesity and dyslipidaemia) and oxidative stress in hepatocarcinogenesis.[4] Oxidative stress is generally recognised as an important factor in hepatocarcinogenesis.[2,6] Our immunohistochemical results showed oxPC-positive steatotic hepatocytes in the background liver tissue of HCC. OxPC, one of the lipid peroxides, is a highly specific marker of oxidative damage. In our previous observation, its immunoreactivity was seen mainly in steatotic or degenerated hepatocytes in NAFLD, and only in some Kupffer cells in normal liver tissues.[5] Hence, the present result suggested that the fatty liver had chronically been exposed to oxidative stress, which was probably initiated prior to hepatocarcinogenesis. To our knowledge, this is the first direct evidence of oxidative hepatocellular injury occurring in simple fatty livers complicated by HCC. Excess fat accumulation itself, even in the absence of inflammation, can be a source of oxidative stress that induces hepatocarcinogenesis. In conclusion, simple steatosis-related oxidative stress should be considered as one of the risk factors of HCC.

Yoshihiro Ikura*
Eiji Mita†
Shoji Nakamori‡

**Department of Pathology, Osaka City University Graduate School of Medicine, Osaka, †Departments of Gastroenterology, and ‡Surgery, National Hospital Organization, Osaka National Hospital, Osaka, Japan*

Contact Dr Y. Ikura.
E-mail: ikura@med.osaka-cu.ac.jp

1. Neuschwander-Tetri BA, Caldwell SH. Nonalcoholic steatohepatitis: summary of an AASLD Single Topic Conference. *Hepatology* 2003; 37: 1202–19.
2. Caldwell SH, Crespo DM, Kang HS, Al-Osaimi AM. Obesity and hepatocellular carcinoma. *Gastroenterology* 2004; 127(Suppl 1): S97–103.
3. Paradis V, Zalinski S, Chelbi E, Guedj N, Degos F, Vilgrain V, *et al.* Hepatocellular carcinomas in patients with metabolic syndrome often develop without significant liver fibrosis: a pathological analysis. *Hepatology* 2009; 49: 851–9.
4. Guzman G, Brunt EM, Petrovic LM, Chejfec G, Layden TJ, Cotler SJ. Does nonalcoholic fatty liver disease predispose patients to hepatocellular carcinoma in the absence of cirrhosis? *Arch Pathol Lab Med* 2008; 132: 1761–6.
5. Ikura Y, Ohsawa M, Suekane T, *et al.* Localization of oxidized phosphatidylcholine in nonalcoholic fatty liver disease: impact on disease progression. *Hepatology* 2006; 43: 506–14.
6. Sasaki Y. Does oxidative stress participate in the development of hepatocellular carcinoma? *J Gastroenterol* 2006; 41: 1135–48.

DOI: 10.1097/PAT.0b013e32834274ec

Benign prostatic glands as a tissue component of testicular teratoma: an uncommon histological finding

Sir,

The occurrence of benign prostatic tissue as a component of testicular teratoma has only been described as a single case report.[1] This may be due to its rare occurrence, as well as the failure of the diagnostic pathologist to recognise glands as prostatic on routine sections and to subsequently confirm this by immunohistochemistry. In our laboratory we utilise Solufix (Tissugen, Australia), a glutaraldehyde-based tissue fixative for routine histology. This agent preserves the spermine content of prostatic secretory granules (PSG) which stain intensely with eosin on routine stains allowing easy recognition of prostatic epithelium.[2]

We present two cases of benign prostatic glandular tissue occurring in two patients with primary testicular tumours; a mature teratoma in a 35-year-old male and a mixed germ cell tumour (30% mature teratoma) in a 39-year-old male. Each patient underwent routine inguinal orchidectomy for a clinically detected testicular mass.

On microscopy, benign gland structures were recognised which were lined by two cell types and bore some resemblance to prostatic acini. These glands were highlighted by their intense eosinophilic PSG (Fig. 1 and 2), and were distributed either singularly or as clusters separated by bland stroma. Lining epithelium showed variable morphology ranging from bland epithelial cells consistent with benign prostatic glands (Fig. 1) to epithelial cells with larger nuclei and prominent nucleoli (Fig. 2), consistent with prostatic intraepithelial neoplasia (PIN). The prostatic nature of the glands was subsequently confirmed by strong diffuse cytoplasmic reactivity with immunohistochemistry for PSA (Dako, USA; Fig. 1 inset) and prostatic acid phosphatase (Dako; not shown). Basal cells were confirmed with immunostaining for high molecular weight cytokeratin 34βE12 (Dako; Fig. 2 inset).

Recognition of the first case prompted a histological review of all testicular teratomas over a 10 year period which included 20 testicular tumours comprising pure teratomas ($n=10$) and mixed germ cell tumours with a mature teratoma component of $>10\%$ ($n=10$). This review identified the second case,

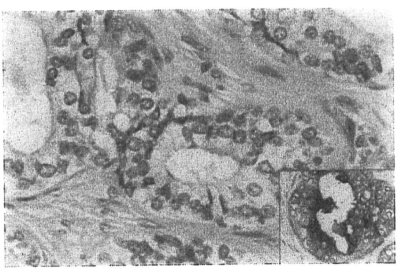

Fig. 1 Benign prostatic glands within a testicular germ cell tumour surrounded by bland stroma. Small eosinophilic granules (prostate secretory granules) are seen in the apical cytoplasm confirming prostatic epithelial differentiation. Inset: These cells are strongly labelled with PSA immunostaining.

Glycobiology vol. 21 no. 2 pp. 235–246, 2011
doi:10.1093/glycob/cwq154
Advance Access publication on October 25, 2010

Expression and the role of 3′-phosphoadenosine 5′-phosphosulfate transporters in human colorectal carcinoma

Shin Kamiyama[2,3,11*], Tomomi Ichimiya[2,*], Yuzuru Ikehara[4], Tomofumi Takase[2], Izumi Fujimoto[2], Takeshi Suda[2], Shoji Nakamori[5], Mitsuru Nakamura[6], Fumiaki Nakayama[7], Tatsuro Irimura[8], Hayao Nakanishi[9], Masahiko Watanabe[10,12], Hisashi Narimatsu[4], and Shoko Nishihara[1,2]

[2]Laboratory of Cell Biology, Department of Bioinformatics, Soka University, 1–236 Tangi-cho, Hachioji, Tokyo 192-8577; [3]Research Association for Biotechnology, 3-9, Nishi-Shinbashi 2-chome, Minato-ku, Tokyo 105-0003; [4]Research Center for Medical Glycoscience (RCMG), National Institute of Advanced Industrial Science and Technology (AIST), 1-1-1 Umezono, Tsukuba, Ibaraki 305-8568; [5]Department of Surgery, Osaka National Hospital, National Hospital Organization, 2-1-14 Houenzaka, Chuo-ku, Osaka 540-0006; [6]East Hospital, Kitasato University, 2-1-1 Asamizodai, Sagamihara, Kanagawa 228-8520; [7]Department of Radiation Emergency Medicine, National Institute of Radiological Sciences, 4-9-1 Anagawa, Inage-ku, Chiba 263-8555; [8]Laboratory of Cancer Biology and Molecular Immunology, Graduate School of Pharmaceutical Sciences, The University of Tokyo, 7-3-1 Hongo, Bunkyo-ku, Tokyo 113-0033; [9]Division of Oncological Pathology, Aichi Cancer Center Research Institute, 1-1 Kanokoden, Chikusa-ku, Nagoya, Aichi 464-8681; and [10]Department of Surgery, School of Medicine, Keio University, 35 Shinanomachi, Shinjuku-ku, 160-8582 Tokyo, Japan

Received on January 31, 2010; revised on September 7, 2010; accepted on September 23, 2010

Sulfation represents an essential modification for various molecules and regulates many biological processes. The sulfation of glycans requires a specific transporter for 3′-phosphoadenosine 5′-phosphosulfate (PAPS) on the Golgi apparatus. This study investigated the expression of PAPS transporter genes in colorectal carcinomas and the significance of Golgi-specific sulfation in the proliferation of colorectal carcinoma cells. The relative amount of *PAPST1* transcripts was found to be higher than those of *PAPST2* in colorectal cancerous tissues. Immunohistochemically, the enhanced expression of PAPST1 was observed in fibroblasts in the vicinity of invasive cancer cells, whereas the expression of PAPST2 was decreased in the epithelial cells. RNA interference of either of the two PAPS transporter genes reduced the extent of sulfation of cellular proteins and cellular proliferation of DLD-1 human colorectal carcinoma cells. Silencing the PAPS transporter genes reduced fibroblast growth factor signaling in DLD-1 cells. These findings indicate that PAPS transporters play a role in the proliferation of colorectal carcinoma cells themselves and take part in a desmoplastic reaction to support cancer growth by controlling their sulfation status.

Keywords: colorectal carcinoma/heparan sulfate/PAPST1/PAPS transporter/sulfation

Introduction

In malignant transformation, specific carbohydrate antigens are expressed on glycoproteins or glycolipids on the surface of cancer cells. Appearance of these carbohydrate epitopes is associated with alterations in the expression of several glycosyltransferases. These carbohydrate epitopes play important roles in the progression and metastasis of cancer cells and are used as typical tumor markers for the diagnosis of various human cancers. In addition, it has been reported that certain nucleotide sugar transporters are involved in the expression of carbohydrate epitopes in cancer. Nucleotide sugar transporters are proteins that are localized on membranes of the endoplasmic reticulum or the Golgi apparatus. These proteins provide substrates for glycosyltransferases in the lumen. Kumamoto et al. (2001) reported that the expression of uridine diphosphate (UDP)-galactose transporter (solute carrier family 35, member A2; SCL35A2) is increased in human colon carcinoma and is responsible for the synthesis of the Thomsen–Friedenreich antigen and sialyl Lewis A (Le^a) and X (Le^x) epitopes. Moriwaki et al. (2007) reported that guanidine diphosphate (GDP)-fucose transporter (SLC35C1) expression is upregulated in hepatocellular carcinoma and plays a role in an increased rate of fucosylation. These reports suggest that the expression of nucleotide sugar transporters is a key factor for regulating the synthesis of carbohydrate epitopes in cancer cells.

Another essential modification is sulfation which is frequently found on the glycans of proteoglycans, glycolipids, and glycoproteins, and on tyrosine residues of proteins. Sulfation is catalyzed by various sulfotransferases, and it modifies the properties of molecules by imparting a negative charge. Heparan sulfate (HS) and chondroitin sulfate (CS) proteoglycans are well-characterized macromolecules that have highly sulfated glycosaminoglycan (GAG) chains and play significant roles in many biological processes. Inhibition of

*The first two authors contributed equally to this article.

[11]Present address: Department of Health and Nutrition, Faculty of Human Life Studies, University of Niigata Prefecture, 471 Ebigase, Higashi-ku, Niigata 950-8680, Japan
[12]Present address: Department of Surgery, School of Medicine, Kitasato University, 1-15-1 Kitasato Sagamihara, Kanagawa 228-8555, Japan
[1]To whom correspondence should be addressed: Tel: +81-42-691-8140; Fax: +81-42-691-8140; e-mail: shoko@soka.ac.jp

sulfation using chlorate, an inhibitor of 3′-phosphoadenosine 5′-phosphosulfate (PAPS) sulfurylase, reduces the signaling of various growth factors such as the fibroblast growth factor (FGF) (Rapraeger et al. 1991; Yayon et al. 1991) and Wnt (Reichsman et al. 1996). Analysis of *Drosophila* mutants with defects in sulfotransferases revealed the importance of sulfation of GAGs on growth factor signaling during development (Lin and Perrimon 1999; Lin et al. 1999; Kamimura et al. 2001, 2006).

On the other hand, it has been reported that some sulfated structures alter the expression of molecules associated with the progression of cancer. Sulfated sialyl Le^x epitopes have been identified as ligands for L-selectin (Mitsuoka et al. 1998), which plays a crucial role in the leukocyte homing process in high endothelial venules. It is known that the risk of malignancy in colorectal cancer is associated with an increase in sialylation (Nakamori et al. 1993; Matsushita et al. 1995; Nakayama et al. 1995) and a decrease in sulfation of carbohydrate epitopes (Yamori et al. 1989; Irimura et al. 1991; Matsushita et al. 1995; Izawa et al. 2000). Immunohistochemical studies have revealed that the goblet cells of human colonic epithelia of Lewis-positive individuals show a strong signal for sulfated mucins (Tsuiji et al. 1998b). The expression of sulfomucins is much lower in colon adenocarcinomas than in the normal mucosa due to the decreased expression of specific sulfotransferases (Seko et al. 2002b).

Two PAPS transporter genes have been previously identified in both humans and *Drosophila* (Kamiyama et al. 2003, 2006; Goda et al. 2006). Lüders et al. (2003) independently reported that *slalom* is a PAPS transporter gene in *Drosophila*. These PAPS transporters are required for the sulfation of cellular proteins and normal development in *Drosophila* (Kamiyama et al. 2003; Lüders et al. 2003; Goda et al. 2006). Additionally, both human PAPST1 (SLC35B2) and PAPST2 (SLC35B3) were found to be involved in the sulfation of the 6-sulfolactosamine epitope in a human colorectal carcinoma cell line (Kamiyama et al. 2006). Huopaniemi et al. (2004) reported that the CMP-sialic acid transporter (SLC35A1), the GDP-fucose transporter (SLC35C1) and the PAPS transporter (SLC35B2) are involved in coordinated transcriptional regulation during induction of sialyl sulfo-Le^x glycan biosynthesis during acute inflammation. These studies indicate that PAPS transporters regulate the sulfation process in addition to sulfotransferases; however, studies have not been conducted on the expression status of PAPS transporter genes in cancer. Therefore, in the present study, we investigated the expression of PAPS transporter genes in colorectal carcinomas and their role in the regulation of sulfation in colorectal carcinoma cells. The significance of Golgi-specific sulfation in proliferation of colorectal carcinoma cells is also discussed.

Results

Expression status of PAPS transporter genes in colorectal carcinomas

Previously, we identified two human PAPS transporter genes: *PAPST1* and *PAPST2* (Kamiyama et al. 2003, 2006). In normal colon tissue, *PAPST1* was expressed at substantially lower level than *PAPST2* (Kamiyama et al. 2006). In the present study, the expression of these PAPS transporter genes in human colorectal carcinomas was investigated. Initially, the expression levels of these transcripts in colorectal carcinoma cell lines were quantified using real-time polymerase chain reaction (PCR). The relative expression level of *PAPST1* transcripts was higher than that of *PAPST2* in all of the 22 colorectal carcinoma cell lines tested (Figure 1A).

Subsequently, the expression levels of *PAPST1* and *PAPST2* were determined in human colorectal tissues. Figure 1B indicates the expression levels of *PAPST1* and *PAPST2* transcripts in cancerous and noncancerous colorectal tissues obtained from seven specimens. Consistent with the result from the cell lines, the relative amount of *PAPST1* transcripts was higher than that of *PAPST2* in colorectal cancerous tissues. Meanwhile, a considerable amount of *PAPST1* transcripts was detected in noncancerous colorectal tissues. In the previous study, we used only one sample for the determination of *PAPST1* and *PAPST2* expression in human colon tissue (Kamiyama et al. 2006). Therefore, the difference might be due to the individual and/or position-specific differences. The expression of *PAPST2* was found to be decreased in colorectal cancerous tissues.

The expression of *PAPST1* mRNA in colorectal carcinoma was confirmed through *in situ* hybridization. As shown in Figure 2A, *PAPST1* mRNA was detected in both adenocarcinoma cells and the stromal cells. To further characterize the distribution of PAPST1 in colorectal tissues, we prepared an antibody against a C-terminal peptide of mouse PAPST1. The immunoreactivity of the anti-PAPST1 antibody to human PAPST1 protein was confirmed by western blot analysis against c-myc-tagged human PAPST1 protein, which was expressed in HEK293 cells (Figure 2C). The anti-PAPST1 antibody specifically recognized both endogenous (Figure 2D, left and middle lanes) and c-myc-tagged human PAPST1 protein (Figure 2D, right lane). Immunohistochemical analysis identified that the predominant expression of PAPST1 is on epithelial cells rather than on stromal cells in both noncancerous (Figure 2E and E′) and cancerous (Figure 2F and F′) colorectal tissues. The expression levels of PAPST1 protein in epithelial cells were similar in cancerous and noncancerous tissues, whereas the observed levels of stromal cells were region-specific and dispersed (Figure 2G, G′ and I, arrows). Moreover, enhanced expression of PAPST1 was also observed in fibroblasts in the vicinity of invasive cancer cells (Figure 2I, asterisks). This suggests that the desmoplastic reaction is associated with elevated levels of PAPST1 in cancerous tissue. PAPST1 protein was detected in all cancerous and noncancerous sections tested in the perinuclear region (Golgi apparatus) of the cells (Figure 2G, G′ and H, arrowheads).

On the other hand, PAPST2 protein was predominantly detected in epithelial cells in noncancerous colorectal tissues (Figure 2J). However, the expression of PAPST2 protein in epithelial cells was faintly detectable in cancerous colorectal tissues (Figure 2K). Strong expression of PAPST2 protein was observed in cells of hematopoietic lineage in both noncancerous and cancerous tissues (Figure 2J and K, diamond arrows). These results indicate that colorectal cancerous tissue increases the expression of PAPST1 in fibroblasts in the vicinity of the desmoplastic reaction and decreases the expression of PAPST2 in epithelial carcinoma cells.

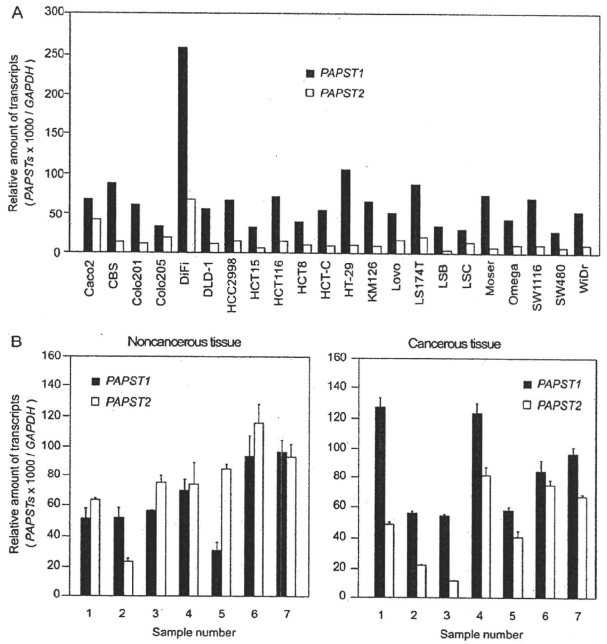

Fig. 1. Quantitative analysis of *PAPST1* and *PAPST2* transcripts in colorectal carcinoma cell lines (**A**) and noncancerous and cancerous human colorectal tissues (**B**). The amounts of *PAPST1* and *PAPST2* transcripts were determined using real-time PCR. The obtained values were normalized with respect to the amount of *GAPDH* transcripts in the same cDNA. Sample information is described in Table I. Left panel, noncancerous tissue, right panel, cancerous tissue.

Table I. Histopathological characteristics of colorectal carcinomas

Sample no.	Site of carcinoma	Histopathological diagnosis
1	Cecum	Moderately differentiated adenocarcinoma
2	Right hemi-colon	Well-differentiated adenocarcinoma
3	Ascending colon	Mucinous adenocarcinoma
4	Sigmoid colon	Moderately differentiated adenocarcinoma
5	Sigmoid colon	Moderately differentiated adenocarcinoma
6	Sigmoid colon	Well-differentiated adenocarcinoma
7	Sigmoid colon	Well-differentiated adenocarcinoma

Sulfated glycoconjugates in colorectal carcinoma cell lines

The sulfation status of cellular proteins in colorectal carcinoma cell lines was investigated using three cell lines, Omega, DLD-1 and LS174T, which were reported as possessing sulfated glycoconjugates (Tsuiji et al. 1998a). These cell lines were metabolically labeled with $Na_2[^{35}S]O_4$ for 24 h and the incorporation of radioactivity into cellular proteins was analyzed (Figure 3A). In all three cell lines, a broad band above 200 kDa was observed (Figure 3A, arrowhead). This signal mostly disappeared when cells were treated with heparitinase, indicating the presence of HS. Omega cells, but not the other two cell lines, exhibited a band at a higher molecular range (Figure 3A, arrow). This signal was derived from CS, as it disappeared upon treatment with chondroitinase ABC. LS174T retained a dense band even after treatment with heparitinase and chondroitinase ABC. Because LS174T is known to have high levels of sulfated mucins (Tsuiji et al. 1998a), this signal was attributed to the sulfated mucins.

The ratio of sulfate incorporation into HS, CS and *N*-glycans was determined in these cell lines. The levels of sulfate incorporation into HS, CS and *N*-glycans were estimated on the basis of the radioactivity released by the treatment of cells or cellular proteins with heparitinase, chondroitinase ABC and PNGase F (peptide:*N*-glycosidase F), respectively. The level of total sulfate incorporation into the proteins was determined from the radioactivity of proteins precipitated with trichloroacetic acid (TCA). Figure 3B shows the ratio of sulfate incorporation into HS, CS, *N*-glycans and

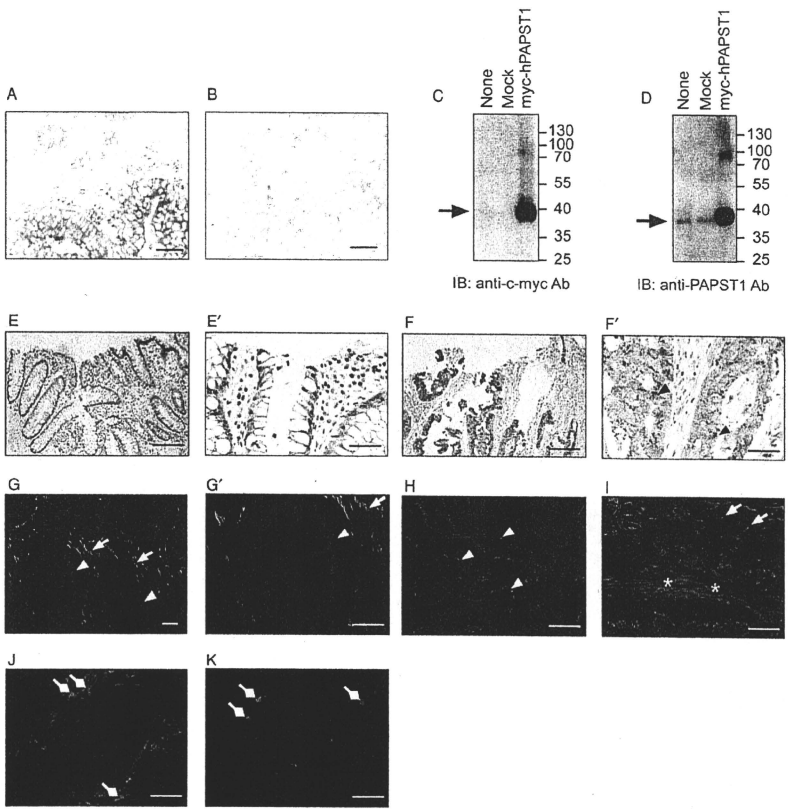

Fig. 2. In situ hybridization of *PAPST1* mRNA and immunohistochemical staining for PAPST1 and PAPST2 proteins in colorectal carcinoma. (**A** and **B**) Serial frozen sections from rectal carcinoma were hybridized with either a digoxigenin-labeled antisense (A) or sense (B) riboprobe against *PAPST1* mRNA. Hybridized probes were detected with an alkaline phosphatase-labeled anti-digoxigenin antibody. Bar scales are 50 μm. (**C** and **D**) The specificity of anti-PAPST1 antibody to human PAPST1 (hPAPST1) protein. A pCXN2-c-myc expression vector containing the *hPAPST1* gene was transfected into HEK293 cells and the cell lysate was prepared. hPAPST1 protein was detected by western blotting using anti-c-myc (C) or anti-PAPST1 (D) antibodies. Arrows indicate the band of hPAPST1 protein. None, intact cells; mock, cells treated with empty vector; myc-hPAPST1, cells treated with pCXN2-c-myc-hPAPST1. IB, immunoblot; Ab, antibody. (**E–F′**) Paraffin-embedded sections were immunostained with anti-PAPST1 antibody using an automated Ventana system. Sections were counterstained with hematoxylin. (E and E′) Noncancerous colorectal tissue and (F and F′) cancerous colorectal tissue. PAPST1 protein was predominantly detected as perinuclear dots in epithelial carcinoma cells (F′, arrowheads). In both noncancerous (E and E′) and cancerous (F and F′) colorectal tissues, stromal cells were weakly stained, whereas epithelial cells were strongly stained. Representative results from 19 (E) and 20 (F) stains are shown. Bar scales are 200 μm (E and F) and 50 μm (E′ and F′). (E and F), low magnification; (E′ and F′), high magnification. (**G–K**) Frozen sections were immunostained with anti-PAPST1 (G–I) or anti-PAPST2 (J and K) antibody and detected with anti-rabbit IgG conjugated Alexa Flour 488 (green). F-actin filaments and nuclei were counterstained with phallotoxin-conjugated Alexa Fluor 594 (red) and with Hoechst 33342 (blue), respectively. (G, G′ and J) Noncancerous colorectal tissues and (H, I and K) cancerous colorectal tissues. In both noncancerous and cancerous colorectal tissues, PAPST1 protein was detected in the perinuclear region (Golgi apparatus) of epithelial cells (G, G′ and H, arrowheads) and stromal cells (G, G′ and I, arrows). Fibroblasts were heavily stained with PAPST1 antibody in the vicinity of invasive cancer cells where the desmoplastic reaction was observed (I, asterisks). PAPST2 protein was strongly detected in cells of hematopoietic lineage (diamond arrows) in both noncancerous (J) and cancerous (K) colorectal tissues. Epithelial cells were stained with anti-PAPST2 antibody in noncancerous colorectal tissues (J), whereas they were only faintly stained in cancerous colorectal tissues (K). Bar scales are 50 μm. (G), low magnification; (G′), high magnification.

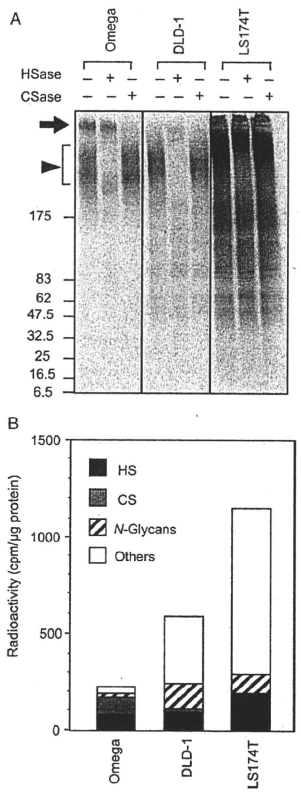

Fig. 3. Metabolic labeling of colorectal carcinoma cell lines. **(A)** Autoradiograph of radioactivity incorporated into cellular proteins. Omega, DLD-1 and LS174T cells were labeled with $Na_2[^{35}S]O_4$ for 24 h and treated in the presence or absence of heparitinase (HSase) or chondroitinase ABC (CSase) for 2 h. Cellular proteins were separated by 2–15% gradient SDS–PAGE. The arrowhead and arrow indicate signals that disappear upon treatment with HSase and CSase, respectively. **(B)** The ratio of sulfate incorporation into HS, CS and *N*-glycans in cellular proteins. The amounts of sulfate incorporated into HS, CS and *N*-glycans were estimated on the basis of the radioactivity released after treatment of cells or cellular proteins with HSase, CSase and PNGase F, respectively. The amount of total sulfate incorporation into proteins was determined by precipitation of the proteins in the cell lysate with TCA.

other glycans. Consistent with the results of autoradiography, Omega cells were found to contain high levels of HS and CS and lower levels of sulfated *N*-glycans. DLD-1 and LS174T cells had low levels of CS but high levels of HS and

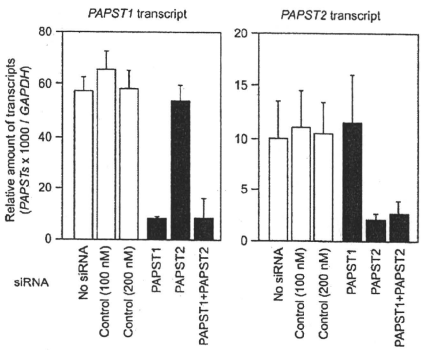

Fig. 4. Knockdown efficiency of each siRNA for *PAPST1* (left panel) and *PAPST2* (right panel) transcripts. Relative amounts of each transcript were quantified using real-time PCR and normalized with respect to the amount of *GAPDH*. Values shown are means (SDs) obtained from three independent experiments. No siRNA, cells treated with no siRNA; control (100 nM), cells treated with 100 nM control siRNA; control (200 nM), cells treated with 200 nM control siRNA; PAPST1, cells treated with 100 nM *PAPST1* siRNA; PAPST2, cells treated with 100 nM *PAPST2* siRNA; PAPST1 + PAPST2, cells treated with 100 nM *PAPST1* siRNA and 100 nM *PAPST2* siRNA.

N-glycans. LS174T contained a substantial amount of extra sulfate, which was considered to be represented by sulfated mucins and sulfated tyrosine residues of proteins.

Gene silencing of PAPS transporters reduces sulfation in DLD-1 cells

To address whether the expression status of PAPS transporters affects sulfation in colorectal carcinomas, the expression of PAPS transporter genes in a colorectal carcinoma cell line was reduced via RNA interference (RNAi). For the RNAi experiments, *PAPST1* siRNA (small interfering RNA), *PAPST2* siRNA and a control siRNA that did not match any human gene were used. On the basis of knockdown efficiency, DLD-1 was selected among the three cell lines. We decided to introduce siRNA in three separate sequential additions because a single addition was found to have a slight effect on the sulfation modification. On days 1, 4 and 7, each of these siRNAs was repeatedly transfected into DLD-1 cells, and the knockdown efficiency was determined by real-time PCR on day 10 (i.e. 3 days after the third transfection). Figure 4 shows the expression of *PAPST1* and *PAPST2* genes in DLD-1 cells treated with each siRNA. Treatment with *PAPST1* and *PAPST2* siRNAs was found to reduce the expression level of the corresponding gene to <20% of the original level. Double knockdown with *PAPST1* and *PAPST2* siRNAs reduced both transcripts in the DLD-1 cells. No significant alteration was observed in the expression level of the nontargeted gene.